DRAFT SF 298

1. Report Date (dd-mm-yy)	2. Report Type	3. Dates covered (from... to)
4. Title & subtitle High Angle of Attack Short Period Flight Control Design with Thrust Vectoring		5a. Contract or Grant #
		5b. Program Element #
6. Author(s)		5c. Project #
		5d. Task #
		5e. Work Unit #
7. Performing Organization Name & Address		8. Performing Organization Report #
9. Sponsoring/Monitoring Agency Name & Address		10. Monitor Acronym
		11. Monitor Report #

12. Distribution/Availability Statement
Distribution approved for Public Release, Distribution Unlimited

13. Supplementary Notes TR downloaded from a WWW unrestricted URL.

14. Abstract

15. Subject Terms

Security Classification of			19. Limitation of Abstract	20. # of Pages	21. Responsible Person (Name and Telephone #)
16. Report Unclass	17. Abstract Unclass	18. This Page Unclass	Unlimited		

High Angle of Attack Short Period Flight Control Design With Thrust Vectoring

Kelly D. Hammett, William C. Reigelsperger, and Siva S. Banda
WL/FIGC, Wright Laboratory
Wright-Patterson AFB, OH 45433-7531

ABSTRACT

A manual flight control system for the short period dynamics of a modern fighter aircraft incorporating thrust vectoring at high angles of attack (α) is presented. Design goals are posed in terms of maintaining acceptable flying qualities during high α maneuvering while also achieving robustness to model parameter variations and unmodeled dynamics. An inner loop dynamic inversion/outer loop structured singular value (μ) - synthesis control structure is used to separately address operating envelope variations and robustness concerns, respectively, eliminating the need for gain scheduling. Angle of attack command following performance objectives are built into both loops. Realistic representations of both structured (real parametric) and unstructured uncertainty are included in the design/analysis process. A flight condition dependent control selector maps generalized controls to physical control deflections, considering actuator redundancy, effectiveness, and saturation issues. Structured singular value analysis, low-order equivalent system (LOES) fits, and linear step responses demonstrate satisfaction of design goals. Effects of including actuator rate and position limits are investigated for an aggressive α doublet command, comparing daisy chained and ganged controls methods. Simulation results suggest a ganged approach offers advantages over daisy chaining at high α.

I INTRODUCTION

This paper details application of the 3 part design approach of Adams et al., 1992, to manual flight control system design for a model of the short period dynamics of the VISTA/MATV F-16 flight test aircraft. The 3 part structure (Fig. 1) consists of an inner loop design that equalizes the dynamics of the plant over the envelope of concern, an outer loop controller that conveniently addresses performance and robustness issues, and a control selector that implements generalized controls, allowing the designer to prioritize and combine control surfaces as desired. For this problem, a modified dynamic inversion formulation (Lane and Stengel, 1988) is chosen to mechanize the inner loop, while μ-synthesis is used to generate the robust outer loop controller, based on the single design plant obtained for all flight conditions by closing the inner loop with assumed perfect inversion. Combining these inner and outer loop design methods avoids gain scheduling (Adams et al), and offers the additional benefit of allowing robustness issues, including robustness to imperfect inversion in the inner loop, to be directly addressed in the μ-synthesis outer loop. The control selector employs the concept of pseudo-controls to facilitate efficient use and combination of control power, and is a "ganged" configuration which distributes commanded pseudo control among all redundant physical controls simultaneously. The control selector also structures the inner loop so that dynamic inversion is readily implemented.

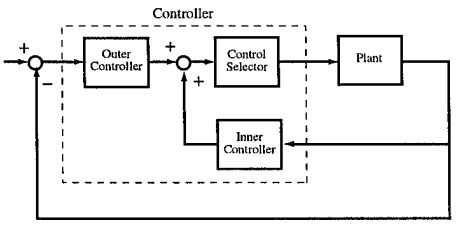

Fig. 1 Three Part Control Structure

Performance objectives for this problem are stated in terms of robust angle of attack command following with desired short period flying qualities. Satisfaction of flying qualities objectives is shown by low order equivalent system fits meeting the requirements of MIL-STD 1797A. Linear step responses demonstrate achieved system tracking performance. Robustness of the design is verified by performing μ–analysis for both structured and unstructured uncertainties over a trim α envelope of 17 to 35 degrees. Finally, a comparison between ganged and daisy chained control selectors to an aggressive α doublet command while including actuator rate and position limits is presented. The simulation results illustrate advantages of control ganging over daisy chaining at high α.

II AIRCRAFT MODEL

Wright Laboratory's Variable Stability In-Flight Simulator Test Aircraft (VISTA) is a modified F-16 with the capability to simulate and test advanced aircraft configurations and flight control concepts. Recently, the VISTA F-16 was modified by the addition of a multi-axis thrust vectoring (MATV) nozzle to facilitate investigation of the tactical utility of high α flight. The MATV nozzle provides additional pitch and yaw control power, primarily for use at high α when traditional aerodynamic surfaces lose effectiveness. A linear model of the VISTA F-16 consisting of decoupled fifth order longitudinal and lateral directional models can be derived assuming a wings level trimmed condition. The longitudinal linear model can be further reduced to the second order short period approximation by removing the altitude and slow phugoid states: velocity and pitch angle. The short period linear model then becomes:

$$\dot{x} = Ax + B\delta \quad \text{or}$$

$$\begin{bmatrix} \dot{\alpha} \\ \dot{q} \end{bmatrix} = A \begin{bmatrix} \alpha \\ q \end{bmatrix} + B \begin{bmatrix} \delta_e \\ \delta_f \\ \delta_{ptv} \end{bmatrix}$$

$$A = \begin{bmatrix} Z_\alpha & 1 \\ M_\alpha & M_q \end{bmatrix}, \quad B = \begin{bmatrix} Z_{\delta_e} & Z_{\delta_f} & Z_{\delta_{ptv}} \\ M_{\delta_e} & M_{\delta_f} & M_{\delta_{ptv}} \end{bmatrix} \quad (2.1)$$

where q is body axis pitch rate, δ_e is elevator (symmetric horizontal tail) deflection, δ_f is symmetric (trailing edge) flap deflection, and δ_{ptv} is pitch thrust vectoring nozzle deflection. Both states are assumed available for feedback. One weight and store configuration, corresponding to two AIM-9 missiles on the wing tips, and the trim throttle setting are assumed.

To illustrate typical high α conditions, a design/analysis point for mach number 0.2 and 10000 ft altitude is considered, corresponding to dynamic pressure of 40.8 psf and 28.0 degree trim α. Linear analysis of this three input, two output system reveals it is controllable from all three inputs individually, but not all the controls are equally effective. At this flight condition thrust vectoring is most effective, while the elevator is slightly less so, and the flaps are relatively ineffective. Further insight into the relative effectiveness and coupling between controls and states can be seen by examining the singular value decomposition (SVD) of the B matrix:

$$B = \begin{bmatrix} -0.04 & -0.03 & -0.05 \\ -1.95 & -0.02 & -2.74 \end{bmatrix} = U\Sigma V^H$$

$$= \begin{bmatrix} -0.02 & 1.00 \\ -1.00 & -0.02 \end{bmatrix} \begin{bmatrix} 3.4 & 0 & 0 \\ 0 & 0.03 & 0 \end{bmatrix} \begin{bmatrix} 0.58 & -0.07 & -0.81 \\ 0.005 & -1.00 & 0.09 \\ 0.82 & 0.06 & 0.58 \end{bmatrix}^H \quad (2.$$

The first right singular vector of B indicates that, neglecting the almost zero (0.005) contribution from the flaps, a combination of positive elevator and positive thrust vectoring in the ratio 0.58 to 0.82 (0.7 to 1.0) produces the maximum obtainable amplification from the control to the state derivative. This gain is 3.4, the maximum singular value of B. The first left singular vector of B shows that the resulting output consists almost entirely of negative pitch rate response. The second columns of the SVD matrices likewise indicate that negative flap deflection is virtually the only way to elicit (positive) response in the $\dot{a}$ channel. Thus, a natural decoupling between states and controls exists for this system. Elevator and thrust vectoring are strong moment producing controls which primarily affect pitch rate, while flaps are very weak direct lift effectors acting primarily on the $\dot{a}$ dynamics.

III PERFORMANCE OBJECTIVES

Performance objectives for this problem consist of robust tracking of pilot angle of attack commands with desired short period flying qualities dynamics as specified in MIL- STD-1797A. Evaluation of flying qualities is performed by obtaining a Low (2nd) Order Equivalent System (LOES) fit of the form in (3.1) to the full model of the closed loop system from commanded to achieved angle of attack:

$$\frac{\alpha}{\alpha_c} = \frac{K\left(s + \frac{1}{T_{\theta 2}}\right)e^{-\tau_\theta s}}{s^2 + 2\zeta_{sp}\omega_{sp}s + \omega_{sp}^2} \qquad (3.1)$$

where K is a gain, $1/T_{\theta 2}$ represents the equivalent system zero, t_q is equivalent time delay, and ω_{sp} and ζ_{sp} are the equivalent short period natural frequency and damping, respectively. In order to achieve Level 1 (Satisfactory) flying qualities for Class IV (High-maneuverability) aircraft, the parameters of (3.1) must fall within the ranges specified below, with V_T representing aircraft total velocity.

$$\omega_{sp} \geq 1 \text{ rad/s} \qquad (3.2)$$

$$0.35 \leq \zeta_{sp} \leq 1.3 \qquad (3.3)$$

$$\tau_\theta \leq 0.1 \text{ s} \qquad (3.4)$$

$$0.28 \leq \frac{\omega_{sp}^2}{(V_T/g)(1/T_{\theta 2})} \leq 3.6 \qquad (3.5)$$

These design goals are injected into the inner and outer loops by specifying ω_{sp} and ζ_{sp} as presented in Sections V and VI. We have chosen the desired ω_{sp} equal to 3 rad/s and desired ζ_{sp} equal to 0.8. Flying qualities evaluation of the complete closed loop system is presented in Section VIII. System robustness objectives are built into the outer loop design model via complex multiplicative plant input uncertainties as described in Section VI. A thorough structured singular value (μ) robustness analysis to multiple real and complex perturbations acting on the system simultaneously is presented in Section VII.

IV CONTROL SELECTOR DESIGN

The primary function of the control selector is to map generalized rate commands into actuator position commands. Using the control selector the designer has direct input into the combination/prioritization of control usage, allowing freedom to address control limits and effectiveness differences. The basic idea is to redefine the control contribution to the state dynamics equation (Haiges et al, 1991),

$$B\delta = B^*\delta^*. \qquad (4.1)$$

B and δ are the actual control effectiveness matrix and control vector, and B^* and δ^* are the generalized equivalents. The actual control can be defined in terms of the generalized control by introducing a transformation matrix, T, such that

$$\delta = T\delta^*. \qquad (4.2)$$

We call T the control selector. It may be calculated as

$$T = N(BN)^{\#}B^*. \qquad (4.3)$$

The operation $(\ )^{\#}$ is a pseudo-inverse and N is a matrix that may be used to combine controls or prioritize individual control channels in the case of redundant effectors. Because the B matrix in (2.1) is a function of flight condition, the control selector is a function of Mach, altitude, and angle of attack.

The generalized inputs for this design are angle of attack rate ($\dot{a}$) command and body axis pitch acceleration ($\dot{q}$) command. The true control inputs are elevator, flap, and thrust vectoring pitch plane nozzle deflections. The actual control effectiveness matrix is given in 2.1 and 2.2, and the generalized control effectiveness matrix is simply the two by two identity matrix:

$$B^* = \begin{bmatrix} 1 & 0 \\ 0 & 1 \end{bmatrix}. \qquad (4.4)$$

Specification of the control weighting/ganging matrix N is now considered. As seen in (2.2), elevator and thrust vectoring are primarily pitch controls, while flaps are mainly α controls. Thus, the assignment of physical to generalized controls is intuitively made for this system: elevator and thrust vectoring to $\dot{q}$ command, and flaps to $\dot{a}$ command. Choosing the proportion of elevator to thrust vectoring in the $\dot{q}$ channel is a more complex issue. The first right singular vector of the B matrix provides a starting point for choosing values based on relative effectiveness. However, actuator dynamics and rate and position limits should also be considered in the choice of N. For this system, the actuators are assumed to possess the transfer functions given below, and the limiting characteristics shown in Table I (Virnig, et al, 1993).

Aerodynamic Effectors:

$$\frac{\delta}{\delta_c} = \frac{(20.2)(144.8)(71.4)^2}{(s+20.2)(s+144.8)\left(s^2 + 2(0.736)(71.4)s + (71.4)^2\right)} \qquad (4.5)$$

Thrust Vectoring Nozzle:

$$\frac{\delta}{\delta_c} = \frac{(21.3)(118.8)(26.3)^2}{(s+21.3)(s+118.8)\left(s^2 + 2(0.444)(26.3)s + (26.3)^2\right)} \qquad (4.6)$$

Table I Actuator Limiting Characteristics

	Aerodynamic Effectors	Thrust Vectoring Nozzle
Rate Limit	± 50 deg/s	± 45 deg/s
Position Limit	± 21 deg	± 17 deg

From (2.2) and this information, it can be seen that although thrust vectoring is slightly more effective than the elevator at this flight condition, it has a slightly slower overall dynamic response and has somewhat more stringent limiting behavior. Since the advantages and disadvantages of each control somewhat balance out, equal weights are chosen, yielding

$$\begin{bmatrix} d_e \\ d_f \\ d_{ptv} \end{bmatrix} = N \begin{bmatrix} d_a \\ \\ d_q \end{bmatrix} \quad N = \begin{bmatrix} 0.0 & 1.0 \\ 1.0 & 0.0 \\ 0.0 & 1.0 \end{bmatrix} \qquad (4.7)$$

which in turn gives a control selector matrix

$$T = \begin{bmatrix} 0.1127 & -0.2154 \\ -32.69 & 0.6484 \\ 0.1127 & -0.2154 \end{bmatrix}. \quad (4.8)$$

The very limited control authority of the flaps observed in (2.2) is also directly evident in (4.8). Table I and the (2,1) element of T indicate that even very small $\dot{a}$ commands will lead to quick flap saturation, preventing achievement of the commanded generalized control. In Section V a method for constraining the $\dot{a}$ command to zero is presented, allowing flaps not to be used and yielding new N and T matrices

$$N = \begin{bmatrix} 0.0 & 1.0 \\ 0.0 & 0.0 \\ 0.0 & 1.0 \end{bmatrix} \quad T = \begin{bmatrix} -0.0042 & -0.2131 \\ 0.0 & 0.0 \\ -0.0042 & -0.2131 \end{bmatrix}. \quad (4.9)$$

Note that the arbitrary choice of equal weights for elevator and thrust vectoring in N leads to equal deflection commands from T. The ramifications of this are briefly explored in Section IX.

V INNER LOOP DESIGN

The inner loop is to equalize the plant dynamics over the operating envelope. Dynamic inversion offers a convenient way to do this, with the extra benefit of allowing specification of desired resulting linear closed loop dynamics. In this paper we use a linearized formulation of the method, keeping linear but flight condition parameter varying equations of motion. Traditional application of dynamic inversion involves choosing the same number of controlled outputs as there are independent controls. Since we desire to control the entire short period dynamics and we have constructed two independent pseudo controls, we choose α and q as the controlled outputs. These variables must only be differentiated once for the controls to appear in the output equations.

$$\begin{bmatrix} \dot{a} \\ \dot{q} \end{bmatrix} = \begin{bmatrix} Z_a & 1 \\ M_a & M_q \end{bmatrix} \begin{bmatrix} a \\ q \end{bmatrix} + \begin{bmatrix} 1 & 0 \\ 0 & 1 \end{bmatrix} \begin{bmatrix} \dot{a}_c \\ \dot{q}_c \end{bmatrix} \quad (5.1)$$

The inverse control law for the inner loop can then be written

$$\begin{bmatrix} \dot{a}_{ci} \\ \dot{q}_{ci} \end{bmatrix} = \begin{bmatrix} 1 & 0 \\ 0 & 1 \end{bmatrix}^{-1} \left(n - \begin{bmatrix} Z_a & 1 \\ M_a & M_q \end{bmatrix} \begin{bmatrix} a \\ q \end{bmatrix} \right) \quad (5.2)$$

where n represents the desired closed loop linear dynamics. Our desired dynamics can be represented by an A matrix with the desired natural frequency and damping multiplying the state:

$$n = A_D x = \begin{bmatrix} a_{D11} & a_{D12} \\ a_{D21} & a_{D22} \end{bmatrix} \begin{bmatrix} a \\ q \end{bmatrix}. \quad (5.3)$$

The inner equalization loop can then be represented as a linear state feedback compensator of the form:

$$\begin{bmatrix} \dot{a}_{ci} \\ \dot{q}_{ci} \end{bmatrix} = K_{eq} \begin{bmatrix} a \\ q \end{bmatrix}$$

$$K_{eq} = \begin{bmatrix} a_{D11} - Z_a & a_{D12} - 1 \\ a_{D21} - M_a & a_{D22} - M_q \end{bmatrix}. \quad (5.4)$$

Using this formulation as is, problems can occur due to the ineffectiveness of the flaps. Equation (5.4) indicates that large differences between a_{D11} and Z_a or a_{D12} and 1 can result in large $\dot{a}_{ci}$ values, in turn leading to large flap deflections and undesirable saturation effects. This effect occurs as a result of our choice of A_D. If possible, we should like to choose A_D so that the first row of K_{eq} is kept near zero, thereby requiring little flap deflection. We also desire to retain the eigenvalues of A_D since they characterize our desired flying qualities dynamics. We achieve our goal by pre and post multiplying A_D by a two by two matrix, M, and its inverse

$$A_d = M A_D M^{-1}. \quad (5.5)$$

If we arbitrarily start with A_D in companion form

$$A_D = \begin{bmatrix} 0 & 1 \\ -w_{sp}^2 & -2z_{sp}w_{sp} \end{bmatrix}, \quad (5.6)$$

Then a simple M which gives the desired result is

$$M = \begin{bmatrix} 1 & 0 \\ -Z_a & 1 \end{bmatrix} \quad (5.7)$$

and now

$$K_{eq} = \begin{bmatrix} 0 & 0 \\ a_{d21} - M_a & a_{d22} - M_q \end{bmatrix}. \quad (5.8)$$

Note that zeros are not worrisome since both the open loop short period and flying qualities systems do not have zeros, and we cannot introduce zeros by applying full state feedback.

VI OUTER LOOP DESIGN

The outer loop compensator is designed to achieve closed loop stability and acceptable flying qualities in the presence of uncertainty. These robust control objectives are met by using a special implicit ideal model following formulation of μ–synthesis. Fig. 2 shows the design model used. The exogenous input is the pilot's α command, and the error signal is created by subtracting the plant's α response from the α response of an ideal model to the same input. As per the controllability issues of Section II, only pitch rate is commanded in the outer loop. The difference between the commanded and achieved a's is the feedback measurement. By block diagram manipulation the system of Fig. 2 can be converted to standard M-D form. The dynamic compensator that yields μ less than or equal to one guarantees robust stability and performance, and is found using a DK-iteration based on the perfectly inverted design plant. The closed inner loop plant equalization ensures this same compensator will achieve design goals for all flight conditions, provided the inversion error is sufficiently small.

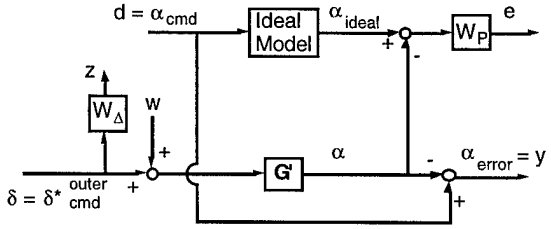

Fig. 2 Design Model for μ–synthesis

The ideal model of Fig. 2 is formed via the LOES transfer function parameters given in Section III:

$$\frac{\alpha}{\alpha_c} = \frac{(3.0)^2}{s^2 + 2(0.8)(3.0)s + (3.0)^2}. \quad (6.1)$$

By forcing the complementary sensitivity function to take the frequency response shape of this ideal model, flying qualities are directly designed for. The performance weight used is:

$$W_p = \frac{0.25s + 50}{s + 5}. \quad (6.2)$$

Uncertainty is modeled entirely as a complex multiplicative perturbation at the plant input with weighting function:

$$W_D = \frac{10(s + 10)}{s + 1000} \quad . \tag{6.3}$$

DK-iteration results in a stable, 6th order controller. Using balanced truncation (Safonov and Chiang, 1988), the outer loop controller is reduced to 4th order. Both the full and reduced order controllers achieve μ less than 1, indicating satisfaction of both stability and performance robustness objectives.

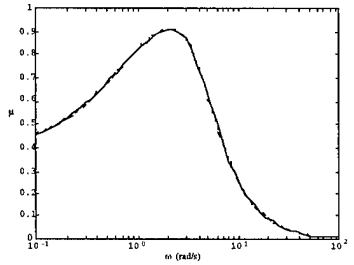

Fig. 3 Closed Loop Structured Singular Value Plot

Implementation of the 3 part controller is shown in Fig. 4. The inner loop controller has inputs of α and q, and generates an inner $\dot{q}$ command. The outer loop controller receives the difference between commanded and achieved a's as input, and outputs an outer $\dot{q}$ command. These two commands are added and passed to the control selector, which transforms the total $\dot{q}$ command into elevator and thrust vectoring deflections. The $\dot{a}$ command and flap deflections have been constrained to zero and do not appear. The equalization gains, K_{eq}, and the control selector, T, are functions of Mach, altitude, and α. The outer loop controller, K_O, is a single fixed dynamic compensator.

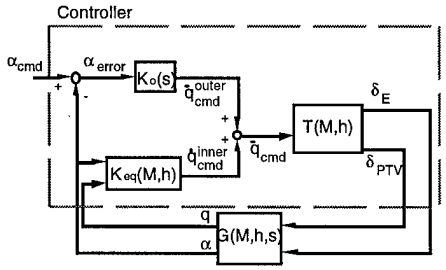

Fig. 4 Controller Implementation

VII ROBUSTNESS ANALYSIS

In this section a model (Fig. 5) reflecting structured and unstructured uncertainty stability robustness requirements is evaluated. The M-D block diagram has inputs and outputs for a structured uncertainty block (w_1 - z_1), an unstructured uncertainty block at the input to the actuators (w_2 - z_2), and an unstructured uncertainty block at the output of the sensors (w_3 - z_3). All perturbations are considered to act simultaneously.

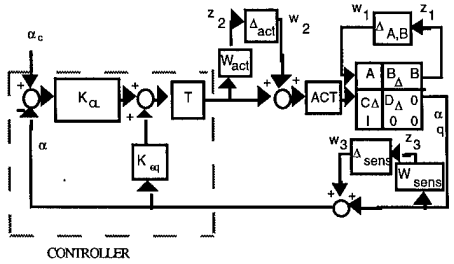

Fig. 5 Robustness Analysis Model

Design structured uncertainty requirements are driven by inner loop equalization errors and perturbations in aerodynamic parameters. Three stability derivatives and four control derivatives are identified for robustness analysis. The level of uncertainty for a parameter is shown in Table II and is captured as a percentage of its nominal value. The A matrix uncertainties allow for large inner loop inversion errors.

Table II : Structured Uncertainty Levels

DZ_a	150%	ΔZ_{de}	20%
DM_a	100%	ΔZ_{dptv}	20%
DM_q	200%	ΔM_{de}	15%
		ΔM_{dptv}	15%

Unstructured uncertainty at the actuator inputs represents both unmodeled dynamics and saturation effects. This uncertainty enters each actuator independently, with weight

$$W_{act} = \frac{10(s + 10)}{s + 1000} \tag{7.1}$$

corresponding to 10 percent error at low frequencies. Sensor uncertainties are low for pitch rate and high for α. This is reflected in the weights used:

$$W_a = \frac{21.9s^2 + 1120s + 91100}{s^2 + 574s + 1140000} \tag{7.2}$$

$$W_q = \frac{0.745s^3 + 152s^2 + 95.9s + 1.38}{s^3 + 626s^2 + 173000s + 235000} \quad . \tag{7.3}$$

Stability robustness is tested for the 28 degree trim α design condition and the 5 off-design conditions given in Table III below. Fig. 6 shows the resulting upper bounds for μ, which are less than one for all frequencies, indicating guaranteed stability for the fairly large set of perturbations considered.

Table III Off-design Analysis Flight Conditions

Test Point	Mach	Altitude (ft)	a (deg)	$\bar{q}$ (psf)
Design	0.2	10,000	28.0	40.8
1	0.25	10,000	16.8	63.7
2	0.18	10,000	35.8	33.0
3	0.25	20,000	26.8	42.6
4	0.3	20,000	17.4	61.3
5	0.35	30,000	20.3	53.9

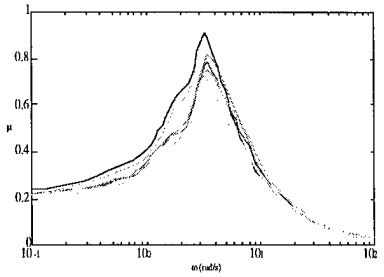

Fig. 6 μ Bounds for Stability Robustness

VIII FLYING QUALITIES EVALUATION

In this section flying qualities are evaluated by fitting a LOES of the form in (3.1) to the full order closed loop transfer function from commanded to achieved α for the 6 flight conditions given in Table III. Figures 7 and 8 show the

evaluation results graphically, indicating that Level 1 flying qualities are achieved at all flight conditions tested.

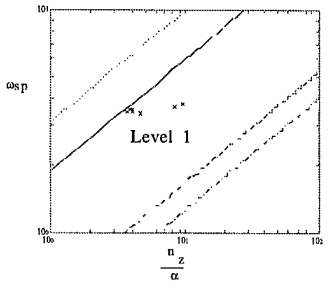

Fig. 7 ω_{sp} vs n_z/a

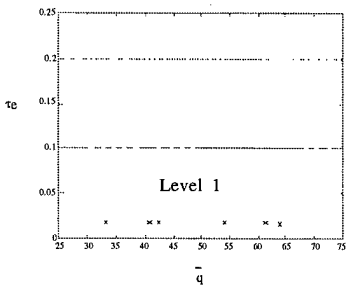

Fig. 8 t_e vs $\bar{q}$

IX SIMULATION RESULTS

Fig. 9 shows unit step α command responses for the linear closed loop and ideal systems for the 28 degree α flight condition. The solid line represents the ideal flying qualities model response, while the dashed line represents the closed loop system response including 4th order actuator models. The time response plot shows that the achieved and ideal linear tracking of α commands are very similar.

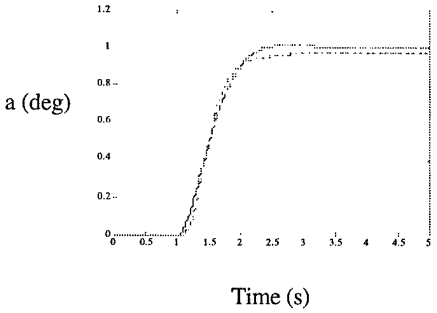

Fig. 9 Ideal vs Achieved Linear Unit Step α Responses

The manual flight control system presented here must eventually exhibit satisfactory properties in a nonlinear environment. Therefore, a brief examination of system behavior while under the control limitations of Table I is conducted. For the same flight condition as above, an aggressive 5 degree up/10 degree down α doublet separated in time by 4 seconds is commanded. Results for two redundant control allocation schemes are presented, with the dashed lines representing ideal and the solid lines representing achieved system response. Fig. 10 shows the response for the ganged control scheme, which commands simultaneous and equal deflections in both elevator and thrust vectoring for a given $\dot{q}$ command. Fig. 11 shows results for a commonly used daisy chained approach (Buffington et al, 1994), which first assigns commanded $\dot{q}$ to the elevator, and then passes any unachieved command on to thrust vectoring. The figures show that the ganged system achieves very good tracking, but the daisy chained system goes unstable trying to follow the second, larger step α command. The instability occurs as a result of additional phase lag produced by the daisy chaining logic (Hammett et al.). The phase lag produced is input amplitude dependent, and thus, as this example shows, using ganged controls at high α permits more aggressive maneuvering.

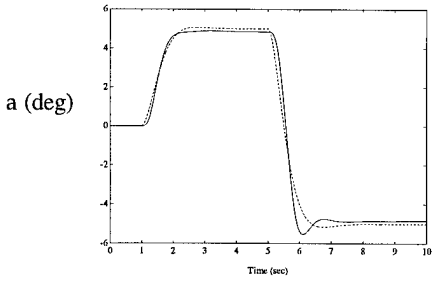

Fig. 10 Ganged vs Ideal Response to α Doublet Command

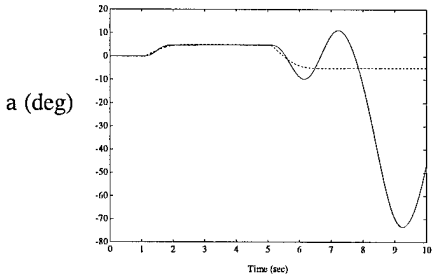

Fig. 11 Daisy Chained vs Ideal α Doublet Command Response

X CONCLUSIONS

A robust flight control design for the short period dynamics of the VISTA/MATV F-16 has been presented which combines linear dynamic inversion and μ–synthesis. An inner/outer loop structure and pseudo-controls are used to achieve performance and robustness goals for a high α flight envelope without gain scheduling. The approach uses a control selector, an inner equalization loop, and an outer robust performance loop to achieve excellent performance and robustness. Simulation results including actuator limits indicate that ganged allocation of physical to generalized controls offers stability and performance advantages over daisy chaining at high α.

REFERENCES

[1] Adams, R. J., et al., "An Introduction to Multivariable Flight Control System Design," WL-TR-92-3110, Oct. 1992.

[2] Buffington, J. M., et al., "Robust, Nonlinear, High Angle-of-Attack Control Design for a Supermaneuverable Vehicle," *Proc. AIAA Guidance and Control Conf.*, Aug., 1993.

[3] Haiges, K. R. et al., "Robust Control Law Development for Modern Aerospace Vehicles," WL-TR-91-3105, Aug. 1991.

[4] Hammett, K. D. et al, "Actuator Limits and Control Allocation at High Angle of Attack - A Short Period Example", submitted to the *AIAA Journal of Guidance, Dynamics, and Control*, July 1994.

[5] Lane, S. H. and Stengel, R. F., "Flight Control Design Using Non-linear Inverse Dynamics," *Automatica*, vol. 24, pp. 471-483, 1988.

[6] "Military Standard - Flying Qualities of Piloted Vehicles," MIL-STD-1797A, Jan. 1990.

[7] Safonov, M. G. and Chiang, R. Y. , "Model Reduction for Robust Control: A Schur Relative Error Method," *International Journal of Adaptive Control and Signal Processing*, vol. 2, pp. 259-272, 1988.

[8] Virnig, J. C., et al., "Application of Multivariable Control Theory to Aircraft Control Laws: Interim Report 1, Definition of Control Problem and Requirements," Nov. 1993.